Selective Reduction of Nitric Oxide over Noble Metals

KATHLEEN C. TAYLOR AND JAMES C. SCHLATTER

Physical Chemistry Department, General Motors Research Laboratories, Warren, Michigan 48090
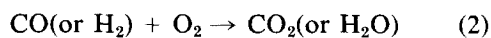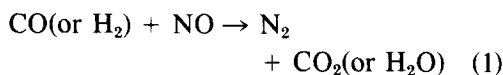
Laboratory studies of the partitioning of CO between NO and O_2 under net lean conditions over the noble metals Ir, Rh, Pt, and Pd showed that over Ir alone is the CO + NO reaction favored over the CO + O_2 reaction. Furthermore, Ir exhibited a particle size dependence such that small Ir crystallites were more effective for reducing NO than large particles. Space velocity experiments showed that NO and O_2 react simultaneously with CO over Ir. NO reduction is positive order in NO concentration under the conditions studied. The NO reaction is enhanced by CO (CO is not inhibiting) but inhibited by competitive adsorption of oxygen. The conversion of oxygen was determined by CO availability and was slightly retarded by NO. A reaction mechanism is proposed for the reduction of NO in the presence of excess O_2 at 550°C. We hypothesize that a different site requirement for NO and O_2 adsorption may be important in determining the selectivity of the catalyst when the number of vacant adsorption sites is limited. Ir differs from Rh in that Ir is able to maintain high NO conversion at elevated temperatures in the presence of excess oxygen. Rh, on the other hand, promotes NO reduction at lower temperatures than does Ir. Rh is expected to make a greater contribution to both CO oxidation and NO reduction during catalyst warmup than Ir. Iridium can be lost from the catalyst under our reaction conditions, presumably via volatilization.

INTRODUCTION

Three-way catalysts, used for the simultaneous conversion of nitric oxide, carbon monoxide, and hydrocarbons in automobile exhaust, are typically operated close to the stoichiometric air/fuel ratio (*1*). Ideally at the stoichiometric exhaust composition sufficient oxygen is present to convert the CO and hydrocarbons, while activity for reducing NO is maintained. We wish to identify catalysts that operate effectively away from the stoichiometric point in order to alleviate the requirement for tight air/fuel ratio control. Furthermore, operation under somewhat leaner than stoichiometric conditions might be desirable for improved oxidation activity. The noble metal containing three-way catalysts begin to lose activity for converting nitric oxide once the exhaust gas becomes net oxidizing. This activity is lost even though the concentration of the reducing agents (CO, H_2, and hydrocarbons) exceeds the concentration of nitric oxide. Oxygen, which is present in excess, competes with NO for reaction with the reducing agents, which are limiting. This competition has been described by Tauster and Murrell (*2*) as the partitioning of the reducing agent between NO and O_2:

$$CO(\text{or } H_2) + NO \rightarrow N_2 + CO_2(\text{or } H_2O) \quad (1)$$

$$CO(\text{or } H_2) + O_2 \rightarrow CO_2(\text{or } H_2O) \quad (2)$$

The selective catalytic reaction of nitric oxide with hydrogen and carbon monoxide in the presence of excess oxygen has been the subject of several recent publications (*2–8*). Jones *et al.* (*3*) have shown that at low temperatures gaseous hydrogen is more effective than CO and will selectively reduce NO over platinum and palladium catalysts. The NO–H_2 reaction was susceptible to poisoning by lead, sulfur, and carbon monoxide (*3*). At elevated temperatures simultaneous CO oxidation and water–gas shift activity influence this selectivity (*3*).

Tauster and Murrell (*2*) have demonstrated that Ir/Al_2O_3 effectively promotes

the NO–CO reaction in the presence of excess oxygen.

Sigg and Wicke (4) have observed a Pd/Ag/Fe/Al$_2$O$_3$ catalyst to exhibit considerable activity for reducing NO in the presence of an excess of oxygen (NO–CO–H$_2$–O$_2$ feedstream). These authors attribute this selective reduction of NO to reduced activity of oxygen provided by the Pd component of this three-component catalyst.

Schlatter and Taylor (5) have found that the activity of a low loaded rhodium on alumina catalyst for promoting the reduction of NO in the presence of excess oxygen was improved by severe thermal aging. Interestingly the catalyst's activity for promoting the CO–O$_2$ reaction was greatly damaged by the thermal aging (5).

Platinum and palladium catalysts were shown to be less effective than the thermally aged rhodium catalyst for reducing NO in the presence of excess oxygen (5). Lester et al. (6) have reported the order of selectivity for NO conversion relative to O$_2$ of fresh catalysts at 500°C to be Ir $\gg$ Rh > Pt.

A kinetic analysis of the reduction of NO by CO in the presence of a stoichiometric excess of oxygen showed how under certain operating conditions (complete CO conversion) the conversion of NO may become independent of noble metal surface area (7, 8).

In this paper we have explored the selectivity of the noble metals for converting NO and O$_2$ as demonstrated by the partitioning of the reducing agents between these two oxidizing agents. The first part of the paper deals with the different selectivity exhibited by the various noble metals and the influence of catalyst metal loading on the selectivity. The second part explores the influence of reactant composition and space velocity on the selectivity of the Ir catalyst. The third part deals with the effect of temperature on the selectivity of the Ir and Rh catalysts.

EXPERIMENTAL

Catalysts

The catalysts were all prepared by impregnation of a γ-alumina support (3-mm-diameter spheres, BET surface area = 96 m^2/g, pellet density = 1.09 g/cm^3) with aqueous solutions of salts of the metals by the incipient wetness technique. The noble metal salts used in the preparation, the metal loadings, and the techniques used to determine the metal loadings of the final catalysts are listed in Table 1. Following

TABLE 1

Catalysts

Noble metal	Metal loading (wt%)	Metal analysis technique	Source of noble metal
Ir/alumina	0.0028	Neutron activation	IrCl$_4$
	0.051	Neutron activation	ROC RIC
Rh/alumina	0.0022	Atomic absorption	RhCl$_3$ · 3H$_2$O
	0.049	Atomic absorption	Ventron
Pd/alumina	0.002	Atomic absorption	5% PdCl$_2$
	0.04	X-Ray fluorescence	Matheson, Coleman and Bell
Pt/alumina	0.002 [a]	Atomic absorption	10% H$_2$PtCl$_6$ · 6H$_2$O
	0.06	X-Ray fluorescence	Baker

[a] Nominal loading.

impregnation the catalysts were dried in air overnight at room temperature, heated slowly in flowing air up to 500°C, and held at 500°C for 4 hr.

Chemisorptions

The state of dispersion of the supported metals was characterized by CO chemisorption measurements. The procedure was basically that proposed by Gruber (9), with certain modifications similar to those of Dalla Betta et al. (10). After pretreatment at 500°C in flowing H_2 (60 min) and O_2 (60 min), the sample was stabilized at room temperature in flowing H_2. A measured volume of CO was injected into the carrier upstream from the catalyst, and a thermal conductivity detector was used to determine the amount of CO removed from the gas stream in passing through the sample chamber. A short (10 min) exposure to O_2 at 500°C was sufficient to remove the adsorbed CO in preparation for a repeat injection. The values reported in Table 2 are averages of at least four injections for each sample; typical precision is ±5% of the listed uptake.

Activity Measurements

The laboratory reactor system used to monitor catalyst behavior has been described previously (11). It includes a feedstream blending section, an integral reactor, and an analytical train. For measurements made at a space velocity of 52,000 hr^{-1} the flow through 15 cm^3 of catalyst was maintained at 13 liters/min (STP). For measurements at a higher space velocity (104,000 hr^{-1}) the catalyst bed volume was decreased to 7.5 cm^3. For measurements at a space velocity of 26,000 hr^{-1} the catalyst bed was increased to 30 cm^3.

The feedstream was blended to provide a range of gas compositions. In each case the concentration of the oxidizing gases (O_2 and NO) was fixed and the concentration of the reducing gas (H_2 or CO) was varied up to the stoichiometric composition. We always included 10 vol% water vapor in the feedstream, a level typical of that in exhaust gas. As a result hydrogen may be available in the NO–O_2–CO feedstream (via catalysis of the water–gas shift reaction: CO + H_2O → H_2 + CO_2) and may also reduce NO and O_2. No H_2 was detected in the reactor effluent. Because the reactant composition was always stoichiometric or leaner, we detected no NH_3 as a product, either (5). Neither CO_2 (~10 vol% in exhaust) nor SO_2 (~20 ppm by volume in exhaust) was included in our feedstreams. SO_2 has been reported to have important effects on three-way reactions, although the effects were more pronounced under rich conditions than under lean conditions such as ours (12). The ranking of the four metals considered here for NO conversion under lean conditions was not affected by the presence of SO_2 (12). The experimental procedure followed in making activity measurements is described below. The catalysts were heated to the reaction temperature (550°C) in the absence of reducing agent (NO, O_2, H_2O, N_2 present). The reducing agent was then admitted at 550°C. The concentration of reducing agent was varied stepwise from 0.1 vol% up to the stoichiometric amount. The midbed temperature was controlled at 550°C. Steady-state outlet concentrations were recorded

TABLE 2

CO Chemisorption Measurements

Metal	Loading (wt%)	CO uptake (μmol/g)[a]	CO/metal atom ratio
Ir	0.0028	0.14	0.96
	0.051	0.74	0.28
Rh	0.0022	0.32	1.5
	0.049	6.77	1.4
Pd	0.002	0.15	0.8
	0.04	2.92	0.8
Pt	0.002[b]	0.16	1.6
	0.06	2.07	0.7

[a] All values have been corrected for the uptake on the blank support, 0.06 μmol/g.

[b] Nominal loading.

for each set of feedstream conditions. In reporting the data the percent conversions of NO, O_2, and CO or H_2 are plotted as a function of the volume percent of CO or H_2 in the feedstream. We also found it to be informative to plot the percent conversion of NO against the percent conversion of O_2. These plots show the selectivity of the catalyst for converting NO and O_2 for various inlet concentrations of the reducing agent.

Activity measurements were also made as a function of catalyst temperature using a fixed feedstream composition. These measurements were not made at steady state. The reactor skin temperature was raised at a rate of 10°C/min from ambient to 625°C. The skin temperature was always greater than the temperature at the reactor inlet. The catalyst temperature was monitored by two thermocouples in the catalyst bed. The temperature read from the thermocouple placed near the bottom of the catalyst bed exceeded the inlet temperature by 30 to 40°C before catalyst lightoff and ~125°C after catalyst lightoff with 1 vol% CO in the feed. The activity data are plotted as a function of the catalyst temperature, as determined with the thermocouple in the center of the catalyst bed.

We also made activity measurements without any catalyst in the reactor in order to determine whether a correction of the data for conversion of O_2 and reducing agents in the reactor preheating section was required. To make the blank measurement we replaced the catalyst bed with silicon carbide. The conversion of O_2, NO, CO, and H_2 for typical feedstream compositions was measured. The results of these measurements are shown in Table 3. Carbon monoxide conversion is only significant be-

TABLE 3

Blank Corrections[a]

I. Feedstream: 0.5 vol% O_2, 0.05 vol% NO, 10 vol% H_2O, variable CO, balance N_2.

CO inlet (vol%)	% of inlet CO converted	Corrected CO inlet (vol%)	Corrected O_2 inlet (vol%)
0.1	17	0.08	0.49
0.2	13	0.17	0.49
0.3	10	0.27	0.49
0.4	7	0.37	0.49
0.5	3	0.48	0.49

II. Feedstream: 0.5 vol% O_2, 0.05 vol% NO, 10 vol% H_2O, variable H_2, balance N_2.

H_2 inlet (vol%)	% of inlet H_2 converted	Corrected H_2 inlet (vol%)	Corrected O_2 inlet (vol%)	Corrected NO inlet (vol%)
0.1	19	0.08	0.49	0.05
0.2	22	0.16	0.48	0.05
0.3	23	0.23	0.47	0.05
0.4	25	0.30	0.45	0.05
0.5	25	0.38	0.44	0.048
0.6	24	0.46	0.43	0.048
0.7	23	0.54	0.42	0.048
0.8	22	0.62	0.41	0.048
0.9	22	0.70	0.40	0.047
1.0	34	0.66	0.33	0.044

[a] Catalyst replaced by silicon carbide. Bed temperature 550°C.

low 0.3 vol% initial concentration. The percentage of hydrogen conversion in the silicon carbide containing reactor was approximately constant even though the initial hydrogen concentration was varied. Later, in Fig. 3, we will demonstrate the effect of applying a correction for the hydrogen, oxygen, and NO conversion by assuming that this conversion simply lowers the inlet concentrations.

This is a complex catalytic system, where large gradients exist not only in temperature and gas stream composition through the catalyst bed, but also in the active metal distribution within the catalyst pellets. It is difficult to assess the importance of possible diffusional influences on the observed conversions. On one hand, since the primary reactants have similar diffusive properties, the degree of diffusion control might be expected to have little effect on the measured selectivity. On the other hand, the availability of CO within the catalyst pellet will depend strongly upon the amount and distribution of the active metal. Insofar as reaction rates and selectivities are dependent upon CO concentration, they could be influenced by metal loadings and impregnation profiles. Since we have no way of isolating reaction kinetics from transport effects in our integral reactor, our discussions relate to the overall reactor response when operating conditions are changed.

RESULTS

Comparison of Ir, Rh, Pt, Pd

The steady-state conversion of NO, CO, and O_2 in the net oxidizing feedstream was determined as a function of initial CO concentration using similarly pretreated samples of each of the noble metal catalysts. The feedstream was chosen to contain a tenfold excess of O_2 over NO in order to reflect the greater O_2 levels versus NO levels in automobile exhaust. Likewise, the feed contained 10 vol% water vapor and the catalyst temperature was set at 550°C.

The results for the 0.0028 wt% Ir/Al_2O_3 catalyst are presented in Fig. 1A. For these particular feedstream conditions and catalyst, the percent conversion of nitric oxide exceeds the percent conversion of oxygen at all initial CO concentrations except at 0.1 vol% CO. Nitric oxide reduction was close to 100% at less than the stoichiometric CO concentration. The oxygen was only 77% reacted at the stoichiometric CO concentration. The activity of this catalyst for NO reduction in a progressively more oxidizing feed may be seen by viewing the figure from right to left.

The oxygen conversions obtained using the paramagnetic oxygen analyzer and the conversions calculated from the CO and NO conversion data always agreed within 5%. The CO conversion reached a maximum of 89% at the 0.3 vol% level then declined to 70% at 1.05 vol% (stoichiometric mixture). It will be shown later that CO actually inhibits NO conversion at lower temperatures (350°C).

The results for the 0.0022 wt% Rh/Al_2O_3 catalyst are presented in Fig. 1B. The activity of the catalyst for converting NO in the presence of excess oxygen is considerably less than the activity exhibited by the Ir catalyst. Up to an initial CO concentration of 0.3 vol% no NO was reduced and only above 0.5 vol% CO did NO reduction become significant.

This catalyst readily promoted the CO + O_2 reaction at all initial concentrations of the reducing agent. The added CO reacted completely in the net oxidizing feedstream, and the reaction of both oxygen and NO was complete at the stoichiometric point.

The results for the 0.002 vol% Pt/Al_2O_3 catalyst are presented in Fig. 1C. Oxygen reacted more readily than NO at low initial CO levels. Above 0.7 vol% initial CO, the CO + O_2 reactivity remained constant (independent of initial CO), and above 0.9 vol% initial CO the NO + CO reactivity showed no further increase. This leveling out of the NO and O_2 conversions is reflected in the data for the conversion of
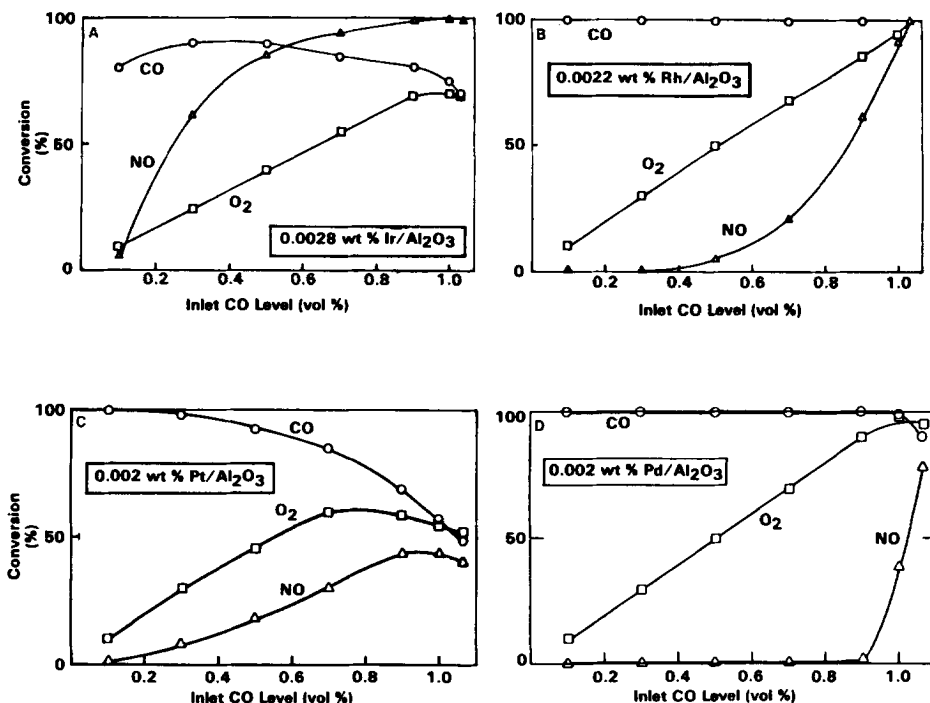
FIG. 1. Conversions of NO, CO, and O_2 over (A) 0.0028 wt% Ir/Al_2O_3; (B) 0.0022 wt% Rh/Al_2O_3; (C) 0.002 wt% Pt/Al_2O_3; and (D) 0.002 wt% Pd/Al_2O_3 at 550°C. Feedstream composition: 0.05 vol% NO, 0.5 vol% O_2, 10 vol% H_2O, 0 to 1.05 vol% CO, and balance N_2. Space velocity: 52,000 hr^{-1} (STP).

CO which reached 100% at an initial concentration of 0.1 vol% but declined thereafter as more CO was added to the feedstream. Thus, at this very low metal concentration, platinum was not as effective as rhodium or palladium for oxidizing CO.

The results for the 0.002 wt% Pd/Al_2O_3 catalyst are presented in Fig. 1D. This Pd/Al_2O_3 catalyst exhibited the smallest selectivity for promoting the NO + CO reaction of the four noble metal catalysts examined here. Essentially no nitric oxide was reduced at any initial CO concentrations up to 0.9 vol%. With 1.0 vol% or more initial CO in the feedstream, the catalyst promoted the reaction of CO with NO; however, at these CO levels most of the oxygen initially present can be removed by the CO + O_2 reaction.

The selectivity of these catalysts for promoting the NO + CO reaction versus the O_2 + CO reaction is compared directly in Fig.

2, which is a plot of percent NO conversion versus percent O_2 conversion. Movement along the curves from left to right is produced by increasing the initial CO concentration in the feedstream. The curve for the Ir catalyst does not extend to the upper-right corner because O_2 did not react completely; the curve for the Pd catalyst does not extend to the upper-right corner because NO did not react completely. The diagonal represents equal percent conversion of NO and O_2. For curves above the diagonal (e.g., Ir) the percent NO reacted at a particular initial CO concentration exceeds the percent O_2 reacted, whereas for curves below the diagonal (e.g., Rh, Pt, Pd) the percent O_2 reacted exceeds the percent NO reacted. This comparison illustrates that while there are differences between the noble metals Pt, Pd, and Rh for reducing NO in a net oxidizing environment, Ir stands alone in its preference for the NO + CO reaction.
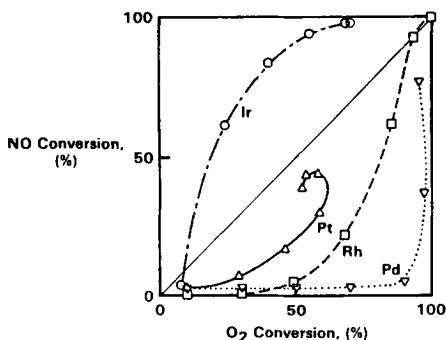
FIG. 2. Comparison of the selectivity of Ir/Al$_2$O$_3$, Rh/Al$_3$O$_3$, Pt/Al$_2$O$_3$, and Pd/Al$_2$O$_3$ for the reactions NO + CO vs O$_2$ + CO. The same data shown in Fig. 1 were used for Fig. 2.

Comparison of CO and H$_2$ Partitioning

Figure 3 contains a comparison of the selectivity of 0.0028 wt% Ir/Al$_2$O$_3$ and 0.0022 wt% Rh/Al$_2$O$_3$ for the reactions H$_2$ + NO versus H$_2$ + O$_2$. In this case, H$_2$ is partitioned between the two oxidizing agents. The blank correction, discussed in the Experimental section, is shown to have only a minor effect on the position of the curves. It has no effect on the interpretation of our results.

The added H$_2$ was completely reacted at all concentration levels examined in these experiments over Rh/Al$_2$O$_3$. Over 0.0028 wt% Ir only 78% of the H$_2$ was reacted when 0.1 vol% H$_2$ was in the feed. The percent conversion of H$_2$ increased with increasing initial H$_2$ to 100% conversion at the stoichiometric point. The exothermicity of the H$_2$ + O$_2$ reaction could be responsible for the increase in conversion here. As was also the case for reduction by CO, the percent NO reacted with H$_2$ exceeds the percent O$_2$ reacted with H$_2$ for the Ir/Al$_2$O$_3$ catalyst (curve falls above the diagonal), whereas for the Rh/Al$_2$O$_3$ catalyst the percent O$_2$ reacted exceeds the percent NO reacted. Comparison of the H$_2$ partitioning data with the CO partitioning data reveals that, over either metal, H$_2$ does not distinguish between NO and O$_2$ as strongly as CO does. Both curves for reduction by H$_2$ are closer to the diagonal than are the curves

for reduction by CO. Accordingly, CO is the preferred reducing agent for enhancing NO reduction in the net oxidizing feedstream with the Ir/Al$_2$O$_3$ catalyst, and H$_2$ is the preferred reducing agent in an otherwise similar feedstream with the Rh/Al$_2$O$_3$ catalyst.

A 0.06 wt% Pt/Al$_2$O$_3$ catalyst was used to compare the partitioning of H$_2$ and CO with Pt. The reduction of O$_2$ exceeded NO reduction when either H$_2$ or CO was the reducing agent (Fig. 4). The crossing of the H$_2$ and CO curves reflects the inability of H$_2$ to reduce more than 25% of the NO even at the stoichiometric point.

The 0.002 wt% Pd/Al$_2$O$_3$ catalyst behaved like Rh in that the H$_2$ + NO reaction was promoted to a greater extent than was the CO + NO reaction under net oxidizing conditions when similar concentrations of reducing agents are compared. These results are shown in a plot of NO conversion versus CO conversion in Fig. 5.

Metal Loading

In other experiments, the effect of catalyst metal loading on the partitioning of the reducing agents was examined. Figure 5 shows that the partitioning of the reducing
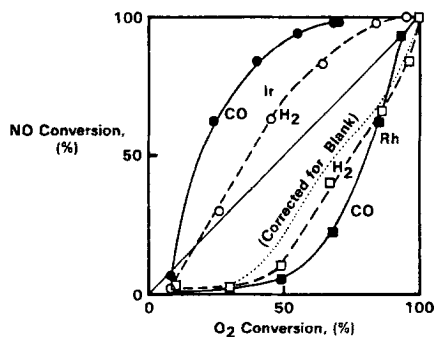

FIG. 3. Comparison of the partitioning of H$_2$ between NO and O$_2$ over 0.0028 wt% Ir/Al$_2$O$_3$ and 0.0022 wt% Rh/Al$_3$O$_3$. The data for CO from Fig. 2 are also plotted here. Feedstream composition: 0.05 vol% NO, 0.5 vol% O$_2$, 10 vol% H$_2$O, either 0 to 1.05 vol% H$_2$ or 0 to 1.05 vol% CO, and balance N$_2$. Space velocity: 52,000 hr^{-1} (STP). Catalyst temperature: 550°C. Dotted line has been corrected for H$_2$ + O$_2$ according to Table 3.
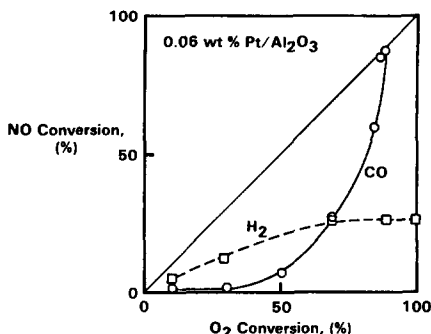
FIG. 4. Comparison of reduction by H_2 and CO over 0.06 wt% Pt/Al$_2$O$_3$. Feedstream: 0.05 vol% NO, 0.5 vol% O$_2$, 10 vol% H$_2$O, 0 to 1.1 vol% H$_2$ or 0 to 1.1 vol% CO, and balance N$_2$. Space velocity: 52,000 hr^{-1} (STP). Catalyst temperature: 550°C.

agents was not changed when the catalyst Pd loading was increased to 0.04 wt%. The chemisorption measurements (Table 2) indicate that the dispersion of Pd on the two catalysts was similar in spite of the 20-fold difference in Pd content. We would not necessarily expect the partitioning to depend on metal loading. A kinetic analysis of a competitive reaction system such as NO–CO–O$_2$ under lean conditions (7, 8) shows that NO conversion is not primarily dependent on metal loading, provided that the temperature is high enough for complete CO conversion.

Pt/Al$_2$O$_3$, Ir/Al$_2$O$_3$, and Rh/Al$_2$O$_3$ all showed changes in partitioning when the metal loading was increased, as evidenced by a shift in the location of the plot of NO versus O$_2$ conversion relative to the diagonal. For example, the 0.002 wt% Pt/Al$_2$O$_3$ catalyst was more selective for NO conversion than the 0.06 wt% Pt/Al$_2$O$_3$ catalyst (Fig. 6). According to the chemisorption data (Table 2) the Pt dispersion on the two catalysts was significantly different. Further work is needed to determine whether the partitioning of CO over Pt/Al$_2$O$_3$ exhibits a metal particle size dependence. The low conversion of both NO and O$_2$ with the 0.002 wt% Pt/Al$_2$O$_3$ catalyst shows that such a small amount of Pt would not contribute significantly to NO and CO conversion. Also, both the CO + O$_2$ and CO + NO

reactions are retarded for CO concentrations close to the stoichiometric amount.

The partitioning of CO and H$_2$ was compared using two Ir catalysts having a 19-fold difference in Ir loading. For the higher loaded 0.051 wt% Ir/Al$_3$O$_3$ catalyst, the partitioning of CO in favor of the NO + CO reaction was less pronounced than for the 0.0028 wt% Ir/Al$_3$O$_3$ catalyst (Fig. 7). Also, the higher loaded Ir/Al$_3$O$_3$ catalyst exhibited less preference for the NO + H$_2$ reaction than did the lower loaded catalyst. In fact, the curve for the partitioning of H$_2$ now falls below the diagonal, which indicates greater selectivity for the H$_2$ + O$_2$ reaction than for the NO + H$_2$ reaction.

We wished to determine whether the partitioning is subject to any particle size effect. Table 2 shows that the 0.051 wt% Ir/Al$_3$O$_3$ catalyst chemisorbed only five times as much CO as did the 0.0028 wt% Ir/Al$_3$O$_3$ catalyst in spite of the higher metal loading. This means that the Ir particle size is much larger on the 0.051 wt% catalyst than on the 0.0028 wt% catalyst. By using four times as much of the 0.0028 wt% Ir/Al$_3$O$_3$ catalyst in the reactor, we were able to compare the partitioning of CO with close to the same number of Ir sites but different particle size. The conversion of NO and O$_2$ was followed as a function of initial CO. The CO was not completely consumed in these experiments. Figure 8
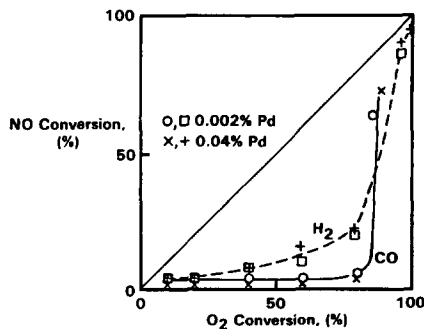

FIG. 5. Comparison of reduction by H_2 and CO over Pd/Al$_2$O$_3$ at two metal loadings. Feedstream composition: 0.1 vol% NO, 1.0 vol% O$_2$, 10 vol% H$_2$O, 0 to 2.1 vol% H$_2$ or CO, and balance N$_2$. Space velocity: 52,000 hr^{-1} (STP). Catalyst temperature: 550°C.
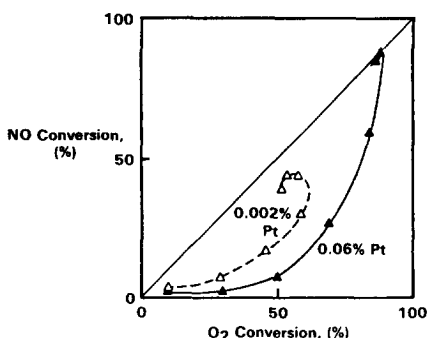
FIG. 6. Effect of Pt loading on the partitioning of CO between NO and O_2. Feedstream composition: 0.05 vol% NO, 0.5 vol% O_2, 10 vol% H_2O, 0 to 1.05 vol% CO, and balance N_2. Space velocity: 52,000 hr^{-1} (STP). Catalyst temperature: 550°C.

shows that over the 0.0028 wt% catalyst considerably more NO was reduced than over the 0.051 wt% Ir catalyst. We suggest then that the greater selectivity of the 0.0028 wt% catalyst may indeed reflect a change in the nature of the catalyst. The NO + CO reaction was enhanced with the 0.0028 wt% catalyst; the CO + O_2 conversion was similar over both catalysts. The enhanced NO conversion, therefore, was not achieved at the expense of decreased O_2 conversion or an increased availability of CO. The partitioning curves are shown in Fig. 9. We cannot rule out the possibility of diffusional influences. We do not think diffusional influences have a major effect on the selectivities since gas-phase diffusivities of NO and O_2 are approximately the same.

We had the opportunity to examine the partitioning at a very low Ir loading when Ir was extensively lost from a catalyst during some early experiments. A 0.0028 wt% Ir/Al$_3$O$_3$ catalyst had been used for approximately 16 experiments at 550°C. Metal analysis revealed that the Ir content had declined to 0.0019 wt%. Figure 10 shows that the decrease in Ir loading was accompanied by a loss of activity for CO + O_2 and a slight shift in the partitioning curve toward the diagonal. We do not know the metal dispersion of the 0.0019 wt% catalyst. We believe the Ir was lost by the

formation of a volatile oxide because Ir is known to react readily with oxygen to form the volatile oxides IrO_2 and IrO_3 at high temperatures (13). We had hoped that the metal loss would have been less severe. We compensated for the problem in subsequent experiments by changing to fresh catalyst samples after every second or third experiment. McVicker et al. (14) have described an approach for preventing sintering by trapping Ir with BaO. Such a method would possibly also prevent volatilization.

The partitioning characteristics of Rh/Al_2O_3 at two metal loadings (0.0022 and 0.049 wt%) are shown in Fig. 11. Just as for the Ir and Pt samples, the lower metal loading tended to be more favorable for NO conversion than the higher loading. Unlike the Ir and Pt, the two Rh catalysts appeared to have similar metal particle sizes (Table 2). These and other aspects of catalysis by Rh under lean conditions will be the subject of a later paper.

Ir/Al_2O_3: Space Velocity

Several experiments were carried out using the 0.0028 wt% Ir/Al$_3$O$_3$ catalyst in which the space velocity was varied. The conversions of NO and O_2 were compared for several initial concentrations of CO. The results obtained for reduction by 0.3
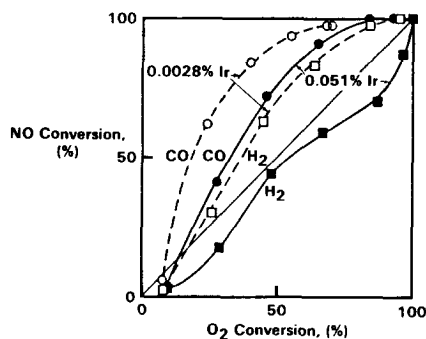

FIG. 7. Effect of Ir loading on the partitioning of CO and H_2 between NO and O_2. Feedstream composition: 0.05 vol% NO, 0.5 vol% O_2, 10 vol% H_2O, 0 to 1.05 vol% CO or H_2, and balance N_2. Space velocity: 52,000 hr^{-1} (STP). Catalyst temperature: 550°C. (O, ●) Reducing agent CO; (□, ■) reducing agent H_2; open symbols 0.0028 wt% Ir; solid symbols 0.051 wt% Ir.
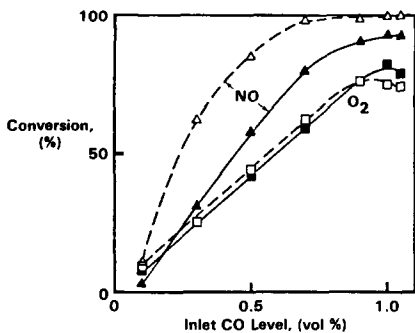
FIG. 8. Effect of Ir particle size. (——) 0.051 wt% Ir/Al$_2$O$_3$, 7.5 cm^3, space velocity 104,000 hr^{-1} (STP). (---) 0.0028 wt% Ir/Al$_2$O$_3$, 30 cm^3, space velocity 26,000 hr^{-1} (STP). Feedstream composition: 0.05 vol% NO, 0.5 vol% O$_2$, variable CO, 10 vol% H$_2$O, and balance N$_2$. Catalyst temperature: 550°C.

and 0.9 vol% CO are given in Figs. 12A and B, respectively. The partitioning of CO between NO and O$_2$ is seen to favor NO conversion at all three space velocities. Because space velocity was changed by changing only the length of the catalyst bed, these graphs indicate the course of the selectivity and net conversion in the integral reactor. With the 7.5-cm^3 catalyst bed size, the CO was not completely reacted at either initial CO level. At 0.9 vol% initial CO and using 15 cm^3 of catalyst, the CO conversion was 80%; the NO was completely reacted but O$_2$ was not. With the 30-cm^3 bed size, additional O$_2$ had time to react with CO. We conclude from the space velocity studies that CO reacts simultaneously with both NO and O$_2$ as the gases
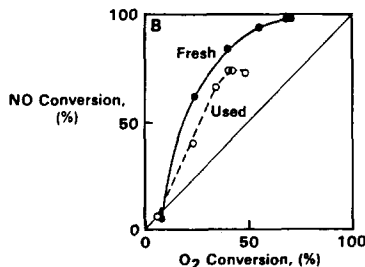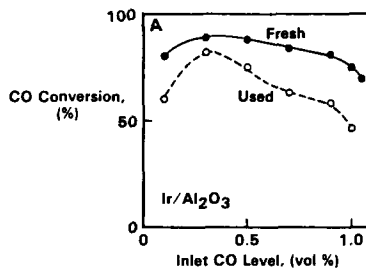

FIG. 10. Effect of prolonged use (16 experiments) on the performance of Ir/Al$_2$O$_3$. (A) CO conversion; (B) NO vs O$_2$ conversion. Feedstream composition: 0.05 vol% NO, 0.5 vol% O$_2$, 10 vol% H$_2$O, 0.1 to 1.1 vol% CO, and balance N$_2$. Space velocity: 52,000 hr^{-1} (STP). Catalyst temperature: 550°C.

progress through the catalyst bed. That is, one gas does not react first followed by the reaction of the other. It is interesting to note that complete NO conversion is achieved before complete CO conversion.

We noted in Fig. 12 that the conversions of CO, NO, and O$_2$ depended both upon the inlet CO concentration and the space veloc-
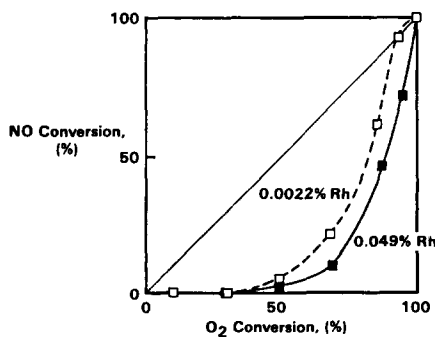

FIG. 9. Partitioning of CO between NO and O$_2$ over 0.0028 wt% Ir/Al$_2$O$_3$ and over 0.051 wt% Ir/Al$_2$O$_3$. Reaction conditions are same as for Fig. 8.

FIG. 11. Effect of Rh loading on the partitioning of CO between NO and O$_2$. Feedstream composition: 0.05 vol% NO, 0.5 vol% O$_2$, 10 vol% H$_2$O, 0 to 1.05 vol% CO, and balance N$_2$. Space velocity: 52,000 hr^{-1} (STP). Catalyst temperature: 550°C.
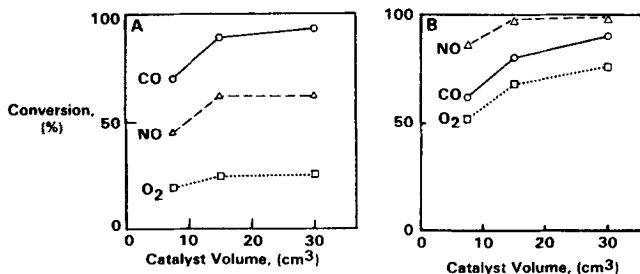
FIG. 12. Effect of space velocity (catalyst bed volume) on the simultaneous reduction of NO and O_2 by CO over 0.0028 wt% Ir/Al$_2$O$_3$ at 550°C. (A) 0.3 vol% initial CO; (B) 0.9 vol% initial CO. Both (A) and (B): 0.5 vol% O_2, 0.05 vol% NO, 10 vol% H_2O, and balance N_2.

ity (bed size). The relationship between the NO and O_2 conversion (i.e., the partitioning curve), however, should *not* depend upon these factors. The governing factor for the NO–O_2 partitioning is the catalyst surface itself, not the residence time in the reactor. For this reason the data for NO conversion versus O_2 conversion fall on practically the same partitioning curve regardless of the space velocity (Fig. 13). An increase in space velocity does decrease the conversions of all three reactants under any given set of inlet concentrations (Fig. 12), but the resulting conversions are constrained to be in accord with the plot in Fig. 13. In other words, any combination of space velocity and inlet CO level which yields, say, 30% conversion of O_2 over the 0.0028 wt% Ir catalyst, will at the same time yield 70% conversion of NO.

Ir/Al$_2$O$_3$: Feedstream Composition

The effect of CO concentration on the partitioning of CO over the 0.0028 wt% Ir/Al$_3$O$_3$ was examined in detail. The reduction of NO and O_2 by CO was compared for three initial O_2 levels as a function of initial CO concentration. The initial CO concentration was varied from 0.1 vol% up to the stoichiometric amount such that the feedstream was net oxidizing except at the stoichiometric point.

Figure 14 shows that for all three levels of O_2 in the feed, the amount of CO reacted is close to the amount of CO in the feedstream, except when the O_2 is only in slight excess. Near the stoichiometric point, the amount of CO reacted changes very little when more CO is added to the reactant stream: CO conversion falls off near the
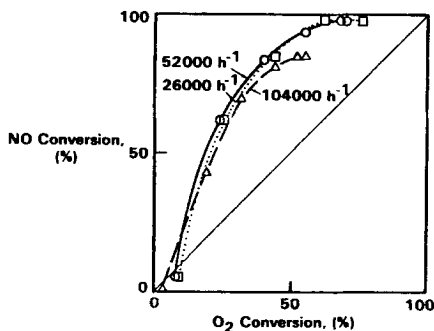

FIG. 13. Effect of space velocity on the partitioning of CO between NO and O_2 over 0.0028 wt% Ir/Al$_2$O$_3$ at 550°C. Feedstream composition: 0.05 vol% NO, 0.5 vol% O_2, 10 vol% H_2O, 0.1 to 1.1 vol% CO, and balance N_2.
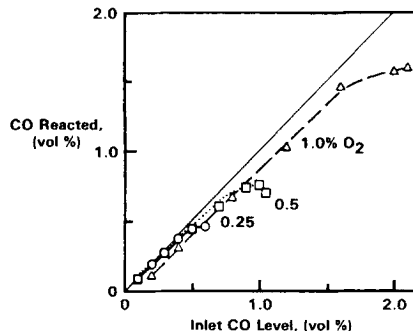
FIG. 14. CO reacted over 0.0028 wt% Ir/Al$_2$O$_3$ at 550°C as a function of initial CO concentration. Feedstream composition: 0.05 vol% NO, 0.25, 0.5, or 1.0 vol% O_2, variable CO, 10 vol% H_2O, and balance N_2. Space velocity: 52,000 hr^{-1} (STP).
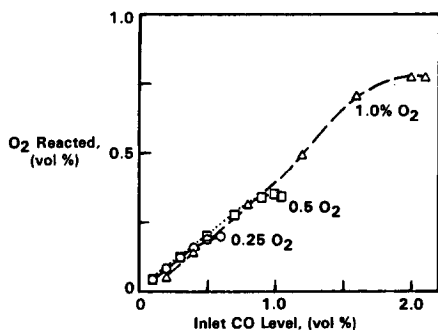
FIG. 15. O_2 conversion over 0.0028 wt% Ir/Al_2O_3 at 550°C as a function of initial CO concentration. Feedstream composition: 0.05 vol% NO, 0.25, 0.5, or 1.0 vol% O_2, variable CO, 10 vol% H_2O, and balance N_2. Space velocity: 52,000 hr^{-1} (STP).

FIG. 17. Effect of initial O_2 concentration on NO reduction by CO in the presence of an excess of O_2. Feedstream composition: 0.05 vol% NO, CO and O_2 as shown, 10 vol% H_2O, and balance N_2. Space velocity: 52,000 hr^{-1} (STP). Catalyst: 0.0028 wt% Ir/Al_2O_3.

stoichiometric point. [This feature of operating under near-stoichiometric conditions has been considered in efforts to design improved three-way catalysts (15).] The amount of CO which reacts with NO is small compared to the amount reacting with O_2; so the plot of O_2 consumption (Fig. 15) mirrors that of CO consumption.

Nitric oxide (0.05 vol%) was also present in the feedstream for the experiments described above. Figure 16 shows that for the conditions used here NO conversion always increased with an increase in the inlet CO concentration; however, greater amounts of CO were required to achieve the same NO conversion at greater initial O_2 concentrations. This effect of initial O_2
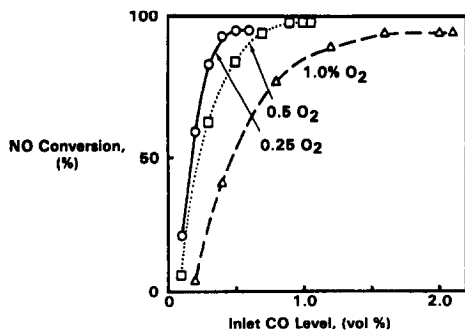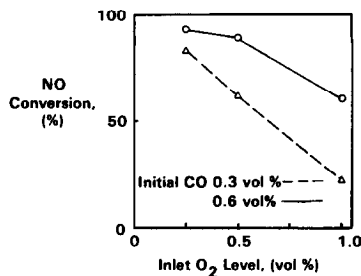
on NO reduction can be seen from plots of NO conversion as a function of initial oxygen concentration (Fig. 17). When the inlet NO and CO concentrations are held constant, an increase in initial O_2 leads to a decrease in NO conversion. This means that a shift to lean (more oxidizing) conditions by increasing the amount of O_2 can be expected to retard NO reduction by CO. We conclude then that either increasing the initial O_2 (CO constant) or decreasing the initial CO (O_2 constant) retards NO reduction over this catalyst. If both CO and O_2 concentrations are increased in the reactant stream, the net effect on NO conversion is relatively small. Table 4, for example, shows the NO conversions resulting from a fourfold change in CO and O_2 levels at a fixed 1:1 molar ratio of these main reactants.

The amount of O_2 reacted with CO was

FIG. 16. NO reduction by CO in the presence of a stoichiometric excess of O_2. Feedstream composition: 0.05 vol% NO, 0.25, 0.5, or 1.0 vol% O_2, variable CO, 10 vol% H_2O, and balance N_2. Space velocity: 52,000 hr^{-1} (STP).

TABLE 4

NO Reduction at $CO/O_2 = 1$[a]

Initial concentrations (vol%)			NO conversion (%)
NO	CO	O_2	
0.05	0.25	0.25	72
0.05	0.5	0.5	84
0.05	1.0	1.0	85

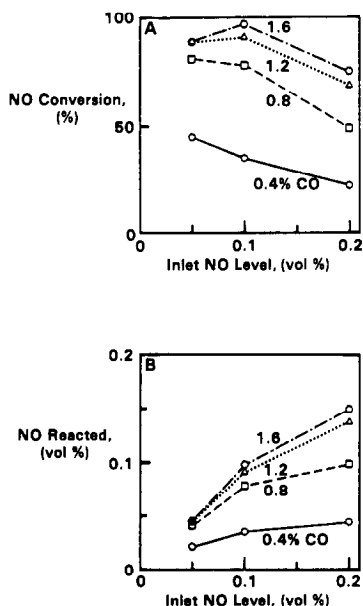[a] 0.0028 wt% Ir/Al_2O_3, 550°C, space velocity 52,000 hr^{-1} (STP).

FIG. 18. Effect of initial NO concentration on NO reduction at various CO concentrations. Feedstream: 1.0 vol% O_2, NO and CO levels as shown, 10 vol% H_2O, and balance N_2. Space velocity: 52,000 hr^{-1} (STP). Catalyst: 0.0028 wt% Ir/Al_2O_3.

found not to be influenced appreciably by initial O_2 concentration. The extent of O_2 reacted was controlled by the amount of CO available to remove it.

To examine the effect of NO concentration on the interactions of CO, O_2, and NO, we used inlet NO levels of 0.05, 0.1, and 0.2 vol%. Within this range, NO conversion decreased as the inlet NO level increased (Fig. 18A) for all the inlet CO levels. Thus, the NO–CO reaction is less than first order in NO under these conditions. Figure 18B shows the reaction to be clearly positive order, though, since the amount reacted increases with inlet NO level.

The effect of NO on the O_2 conversion is shown in Fig. 19 for various CO levels. The effect is small and in a generally negative direction with increasing NO concentration. Large effects were not anticipated, since the O_2 was in considerable excess over the NO.

Effect of Temperature

Experiments were carried out which ex-

plored the partitioning of CO between NO and O_2 at low catalyst temperatures. Experimental conditions were chosen to be similar to those used for previous experiments in that the NO and O_2 concentrations were fixed at 0.05 and 0.5 vol%, respectively. Three initial CO concentrations were compared in separate experiments. The temperature was raised slowly (10°C/min), and conversions were monitored simultaneously. The reactions of O_2 and NO with CO at approximately 350°C (temperature measured near the center of the catalyst bed) are compared in Fig. 20A. This relatively low temperature was chosen for comparison because it reflects the initial stages of the reactions. The decrease in NO and O_2 conversion with an increase in the initial CO concentration reveals that the higher CO level suppresses both reactions. This is in spite of the fact that at the lower initial CO level, the feed composition is more oxidizing (higher O_2/CO ratio). This result suggests that during warm-up NO conversion over such an Ir catalyst can indeed be greater under net lean conditions (net oxidizing) than at the stoichiometric point if the lean conditions are achieved by a reduction in CO concentration in the feed.

Figure 20B shows corresponding data for a catalyst temperature of 450°C, where the CO conversion was nearly complete. Comparison of Figs. 20A and B reveals that, whereas CO inhibits the reactions at low
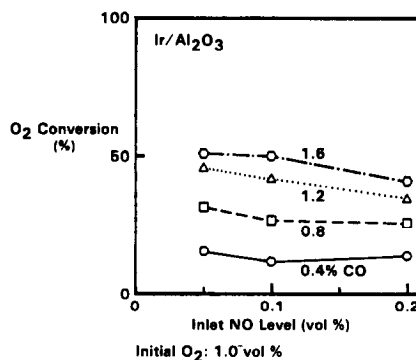

FIG. 19. Effect of initial NO concentration on O_2 reduction at various CO concentrations. Conditions same as for Fig. 18.
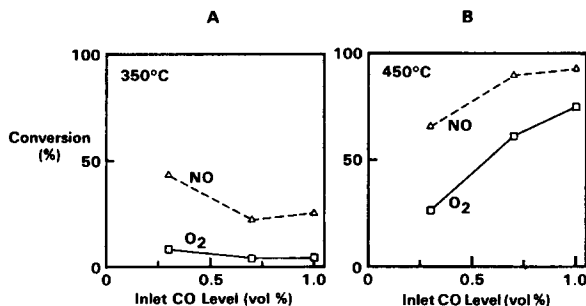
FIG. 20. Partitioning of CO between NO and O_2 at 350 and 450°C (catalyst bed temperature). Feedstream composition: 0.05 vol% NO, 0.5 vol% O_2, variable CO, 10 vol% H_2O, and balance N_2. Space velocity: 52,000 hr^{-1} (STP). Catalyst: 0.0028 wt% Ir/Al_2O_3.

temperature, the conversions of NO and O_2 are markedly enhanced by CO addition at the higher temperature.

Another aspect of the NO conversion efficiency as a function of temperature and CO concentration over this Ir/Al_2O_3 catalyst is depicted in Fig. 21. The figure shows that for an inlet CO level of 0.3 vol%, the NO conversion goes through a maximum at a bed temperature of about 400°C and then declines as the temperature is increased further. The decreased contact time which results from the increased temperature cannot explain the decline in NO conversion; Fig. 12A showed that the conversions were insensitive to contact time (i.e., catalyst volume) in the range of interest. Furthermore, CO conversion did not show such a trend. A maximum in the NO conversion with increasing temperature is not unusual;
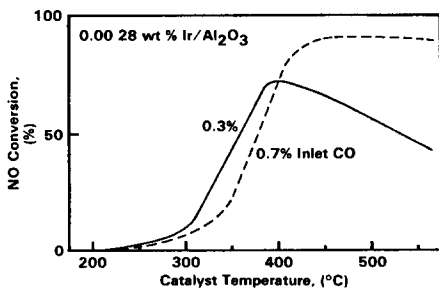

FIG. 21. Temperature dependence of NO reduction over 0.0028 wt% Ir/Al_2O_3 at two inlet CO levels. Both feedstreams contain 0.05 vol% NO, 0.5 vol% O_2, 10 vol% H_2O, and balance N_2. Space velocity: 52,000 hr^{-1} (STP).

a somewhat similar result was reported by Jones et al. (3) for a Pt-containing catalyst. Also we observed only a very small conversion of CO in the reactor inlet (Table 3) so it does not appear that the decrease in NO conversion with temperature is due to a decrease in available CO.

The reduction of NO and O_2 by CO over the 0.0022 wt% Rh/Al_2O_3 catalyst was not suppressed by CO at low temperature as were these reactions over the Ir catalyst. Figure 22 shows the effect of initial CO concentration on NO reduction at catalyst temperatures of 250 and 300°C. Both O_2 and NO conversions increased as the CO concentration in the net oxidizing feed was increased. At these temperatures CO conversion was incomplete (reached 100% at about 350°C). We also note that the percent of NO conversion and percent O_2 conversion are approximately the same at each inlet CO level. The partitioning of the reducing agent in favor of O_2 conversion, which was observed for the studies made at 550°C (Fig. 1B), is then only characteristic of catalyst operation at high temperature.

Experiments that explored the influence of temperature on the reduction of NO and O_2 by CO with the 0.0022 wt% Rh/Al_2O_3 catalyst showed (Fig. 23) that NO reduction began at lower temperatures than with the Ir/Al_2O_3 catalyst (cf. Fig. 21). Figure 23 also shows that the conversion versus temperature plots exhibited a maximum with temperature at all three inlet CO levels. The
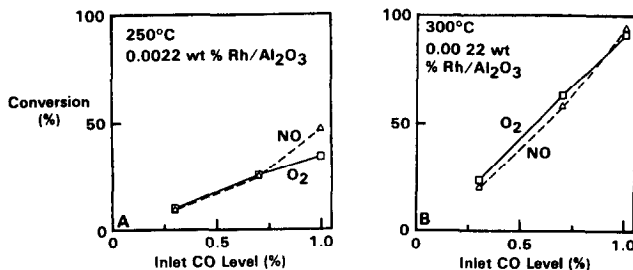
FIG. 22. Partitioning of CO between NO and O_2 at 250 and 300°C (catalyst bed temperature). Feedstream composition: 0.05 vol% NO, 0.5 vol% O_2, variable CO, 10 vol% H_2O, and balance N_2. Space velocity: 52,000 hr^{-1} (STP). Catalyst: 0.0022 wt% Rh/Al_3O_3.

activity data could be reproduced; the decline in activity at high temperature was not due to an irreversible change in the catalyst. The maximum in the conversion–temperature plots suggests that NO conversion under net oxidizing conditions over such a Rh/Al_2O_3 catalyst would be penalized by high-temperature operation even close to the stoichiometric point. The temperature dependence of the partitioning of CO at complete CO conversion suggests that optimal NO conversion under net lean (net oxidizing) conditions would require careful control of catalyst temperature.

DISCUSSION

The results of Fig. 2 illustrate the unique catalytic activity of Ir to promote the reduction of NO to N_2 under net oxidizing conditions and at relatively high temperature (550°C). Because the experiments were carried out by changing the concentration of
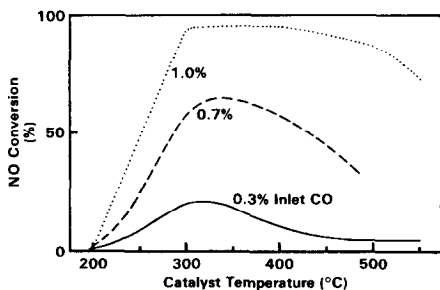

FIG. 23. Temperature dependence of NO reduction over 0.0022 wt% Rh/Al_3O_3 at three inlet CO levels. All feedstreams contain 0.05 vol% NO, 0.5 vol% O_2, 10 vol% H_2O, and balance N_2. Space velocity: 52,000 hr^{-1} (STP).

the reducing agent, the partitioning curve demonstrates the selectivity characteristics for a range of stoichiometries. In particular, the Ir/Al_2O_3 catalyst promoted the NO and CO reaction to a greater extent than did the other noble metals at low CO concentrations. This ability to promote NO reduction at high O_2/CO ratios is the feature of the Ir catalyst which would make it a desirable component of an automobile exhaust catalyst; however, low Ir availability and ready formation of volatile oxides of Ir (as evidenced by Ir loss from the catalysts during prolonged use) require consideration. In fact, loss of Ir from the catalyst may indeed contribute to the loss of activity following thermal aging (10 hr at 1093°C in 10% H_2O–90% air) of an Ir catalyst reported by Lester et al. (6).

Tauster and Murrell (2) reported an apparent metal crystallize size effect on the partitioning of CO between NO and O_2 when Ir/Al_2O_3 catalysts containing 0.1 wt% Ir and 0.001 wt% Ir were compared using a fixed feed composition and variable temperature. The partitioning was followed from the onset of NO reduction until more than 90% of the NO was reacted. In the low-temperature region, inhibition by adsorbed reactants such as CO is likely to occur. Our experiments were carried out at high temperature (550°C) where the reaction is no longer limited by adsorbed CO. Nonetheless, the different partitioning observed with the 0.0028 wt% Ir/Al_2O_3 and 0.051 wt% Ir/Al_2O_3 catalysts resembles the work of Tauster and Murrell (2) in that the

lower Ir containing catalyst was more selective for NO reduction than was the higher Ir containing catalyst. Furthermore, the chemisorption measurements verify that the metal particle size is different for the two catalysts, the higher 0.051 wt% Ir/Al_2O_3 having the larger metal particle size.

The relative ease with which Ir (supported on alumina) sinters complicates studies of crystallite size effects because the reaction temperatures used here exceed the temperature where McVicker et al. (14) report extensive growth in Ir crystallite size. Prolonged use of the 0.0028 wt% Ir/Al_2O_3 catalyst at 550°C has been shown here to decrease the ratio of NO/O_2 reacted compared with a fresh catalyst sample. We attribute this change to sintering of Ir which accompanied metal loss, though the metal area was too low to measure metal dispersion. McVicker et al. (4) have suggested that sintering of Ir/Al_2O_3 is controlled by the formation of an iridium oxide species (perhaps IrO_3).

Figures 21 and 23 show that the higher CO levels inhibit NO reduction at low temperatures with Ir/Al_2O_3, whereas with Rh/Al_2O_3 CO is less inhibiting. In accord with this observation, we found Ir/Al_2O_3 to be a poorer catalyst than Rh/Al_2O_3 for NO reduction under net reducing (excess CO) conditions.

The experiments investigating the dependence upon feedstream composition of the reduction of NO and O_2 over 0.0028 wt% Ir/Al_2O_3 revealed several interesting features of these reactions. The reduction of NO was inhibited by increasing O_2 pressures, as might be expected if O_2 and NO compete for the same surface sites.

Table 4 showed, however, that NO reduction was independent of O_2 concentration so long as the CO/O_2 ratio was constant. This result suggests that the availability of surface sites for NO adsorption/decomposition is controlled by the CO/O_2 ratio. We might consider a mechanism for NO reduction in the pres-

ence of an excess of O_2 whereby both NO and O_2 deposit oxygen on the catalyst and oxygen is only removed by reaction with CO. Such a mechanism is supported by XPS and UPS studies of CO oxidation by NO on Ir(111) (16, 17). Zhdan et al. (16) showed that above 100°C NO decomposed rapidly on Ir to yield chemisorbed nitrogen and oxygen species. When equal partial pressures of NO and CO were admitted to the vacuum chamber at 297°C the intensity of the atomic oxygen peak decreased while the intensity of the atomic nitrogen peak increased (16). At 200°C an oxygen peak attributed to adsorbed CO was found; at 400°C only adsorbed atomic nitrogen and oxygen were observed (molecular NO and CO absent) (17). Kanski and Rhodin (18) have looked at the influence of surface geometry on the chemical nature of the bonding and reaction of NO on Ir. Partial dissociation of NO was observed by UPS on both the Ir(100) and Ir(111) surfaces at 27°C (18). These authors argue that the lower 2π bonding energy on Ir compared with Pt is consistent with partial dissociation of NO on Ir and molecular NO adsorption on Pt.

The ability of Ir to adsorb and dissociate NO in the presence of excess oxygen undoubtedly is a key step in the conversion of NO to N_2 on this catalyst. To date no research has appeared in the literature which provides information on the mechanism whereby adsorbed nitrogen species are converted to nitrogen gas. Campbell and White (19) have discussed two possible mechanisms with rhodium: by one process diffusion of adsorbed nitrogen atoms leads to N_2 formation and N_2 desorption; by another model N_2 is produced in a reaction between adjacent NO (adsorbed) and N (adsorbed). The first model requires vacant nearest neighbor sites for NO dissociation whereas the second model does not.

In Fig. 18B we observed that nitrogen formation over the 0.0028 wt% Ir/Al_2O_3 catalyst was increased when the initial NO concentration was increased. This relation-

ship to gas-phase concentration suggests a mechanism whereby the surface is not saturated with NO (adsorbed) or N (adsorbed) so that gas-phase concentration influences the conversion.

The reaction of O_2 with CO over 0.0028 wt% Ir/Al_2O_3 was not influenced by changes in the initial O_2 concentration, as would be expected with feedstreams deficient in CO. Nitric oxide had a slight inhibiting effect on oxygen conversion. This result suggests that NO can compete successfully with oxygen for surface sites. This observation is supported by the large difference in the sticking probability reported for these gases on Ir(111): near unity for NO (18) and 0.05 for O_2 (20) at ambient temperatures.

The maximum in the NO conversion versus temperature plot for Ir/Al_2O_3 (Fig. 21) compared with Rh/Al_2O_3 (Fig. 23) points to a significant difference in the selectivity of these two catalysts for promoting NO reduction in the presence of excess oxygen (though with the 0.0028 wt% Ir/Al_2O_3 catalyst the maximum disappeared at higher CO levels). We propose that at high temperatures the following reaction scheme is compatible with the data.

Under reaction conditions the surface is populated by oxygen species (derived from both O_2 and NO). The reaction of CO with surface oxygen generates surface sites for further adsorption of NO and oxygen. This is essentially the scheme Tauster and Murrell (2) proposed. The partitioning of CO between NO and O_2 is defined by the origin of the surface oxygen. For partitioning in favor of NO conversion, the fraction of the gas-phase NO that provides surface oxygen is greater than the fraction of the gas-phase O_2 that provides surface oxygen.

We consider the possibility that O_2 chemisorption requires two statistically independent sites whereas NO does not. We propose that NO can adsorb on a single site and wait for an available adjacent site for dissociation and that O_2 adsorption requires simultaneously available adjacent surface

sites. Tauster and Murrell (2) decided that different site configurations were not required in view of their observation that the selectivity of NO reduction did not decrease with an increase in catalyst temperature and because their 0.001 wt% Ir/Al_2O_3 catalyst gave roughly the same conversions (of NO, O_2, or CO) at 500°C as did their 0.1 wt% Ir/Al_2O_3 catalyst at 400°C. We observed that the selectivity for NO reduction over 0.0028 wt% Ir/Al_2O_3 was decreased with an increase in temperature, but only under certain conditions. These conditions were temperatures above 400°C and low CO/O_2 ratios, although the particular conditions depend upon the catalyst being tested (cf. Figs. 21 and 24). We consider the requirement for statistically different sites for O_2 chemisorption but not for NO chemisorption is supported by our observation of the temperature dependence of NO selectivity. We are proposing that the increased temperatures enhance the reaction of CO with surface oxygen and decrease the population of surface oxygen. Accordingly, the availability of "adjacent" surface sites required for O_2 chemisorption is increased. We cannot explain the maximum in the NO conversion versus temperature data by a decrease in CO adsorption since CO conversion was not depressed at elevated temperatures. A decrease in NO chemisorption at elevated temperatures, however, would be expected to lead to lower NO conversion.
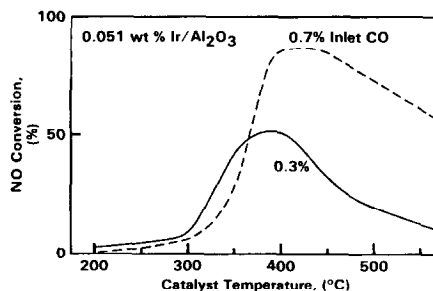

FIG. 24. Temperature dependence of NO reduction over 0.051 wt% Ir/Al_2O_3 at two inlet CO levels. Both feedstreams contain 0.05 vol% NO, 0.5 vol% O_2, 10 vol% H_2O, and balance N_2. Space velocity: 52,000 hr^{-1} (STP).

The observation that catalyst selectivity for NO reduction did not decline with increasing temperature when the initial CO concentration in the feedstream was increased (to 0.7 vol% for 0.0028 wt% Ir/Al_2O_3) requires further discussion. One might predict that the higher CO level would simply lead to greater removal of surface oxygen and less selectivity for NO removal; just the opposite was found (Fig. 21). Upon increasing the initial CO concentration from 0.3 to 0.7 vol%, NO conversion increased. We speculate that at the higher CO level, CO adsorption on the Ir surface might be sufficient to decrease the availability of adjacent sites needed for O_2 chemisorption. This could shift the selectivity to favor NO reduction because single sites needed for NO chemisorption would still be available. The measurements reported by Tauster and Murrell (2) were done at a sufficiently high CO level and perhaps *not* so high a temperature that a falloff in NO conversion with temperature was found.

So far we have said little about the CO + O_2 activity of the Ir/Al_2O_3 catalysts. We hypothesize that differences in catalyst activity for O removal by CO might accompany selectivity differences among the Ir/Al_2O_3 catalyst for the partitioning of CO. Also, we consider the different partitioning of the reducing agent observed when H_2 was substituted for CO to reflect both the possible importance of oxygen removal by the reducing agent for the partitioning and possibly the absence of any inhibiting effect of H_2 on O_2 adsorption on Ir as we suggested for the CO-containing feedstream.

We are not able to say from the experiments we report here whether the different selectivity exhibited by small Ir particles relative to large Ir particles arises from a difference in the interaction of NO and/or oxygen with Ir or a difference in the interaction of CO with the catalysts. The results could be explained by either an increase in the NO interaction or a decrease in the interaction of O_2. The effect of inlet CO concentration on NO conversion at high temperatures (Figs. 21 and 24) suggests that differences in the interaction of CO with the Ir depending upon the particle size could also contribute to the partitioning.

REFERENCES

1. Canale, R. P., Winegarden, S. R., Carlson, C. R., and Miles, D. L., presented at Soc. Auto. Eng. Cong., Detroit, Mich., March 1978, paper 780205.
2. Tauster, S. J., and Murrell, L. L., *J. Catal.* **41,** 192 (1976).
3. Jones, J. H., Kummer, J. T., Otto, K., Shelef, M., and Weaver, E. E., *Environ. Sci. Technol.* **5,** 790 (1971).
4. Sigg, R., and Wicke, E., *Z. Phys. Chem. N.F.* **103,** 181 (1976).
5. Schlatter, J. C., and Taylor, K. C., *J. Catal.* **49,** 42 (1977).
6. Lester, G. R., Joy, G. C., and Brennan, J. F., presented at Soc. Auto. Eng. Cong., Detroit, Mich., March 1978, paper 780202.
7. Tauster, S. J., and Murrell, L. L., *J. Catal.* **53,** 260 (1978).
8. Hegedus, L. L., Herz, R. K., Oh, S. H., and Aris, R., *J. Catal.* **57,** 513 (1979).
9. Gruber, H. L., *Anal. Chem.* **34,** 1828 (1962).
10. Dalla Betta, R. A., McCune, R. C., and Sprys, J. W., *Ind. Eng. Chem. Prod. Res. Develop.* **15,** 169 (1976).
11. Schlatter, J. C., presented at Soc. Auto. Eng. Cong., Detroit, Mich., March 1978, paper 780199. Research Publication GMR-2566.
12. Summers, J. C., and Baron, K., *J. Catal.* **57,** 380 (1979).
13. Jehn, H., Volker, R., and Ismail, M. I., *Platinum Metals Rev.* **22,** 92 (1978).
14. McVicker, G. B., Garten, R. L., and Baker, R. T. K., *J. Catal.* **54,** 129 (1978).
15. Hegedus, L. L., Summers, J. C., Schlatter, J. C., and Baron, K., *J. Catal.* **56,** 321 (1979).
16. Zhdan, P. A., Boreskov, G. K., Egelhoff, W. F., Jr., and Weinberg, W. H., *J. Catal.* **45,** 281 (1976).
17. Zhdan, P. A., Boreskov, G. K., Boronin, A. I.,

Schepelin, A. P., Egelhoff, W. F., Jr., and Weinberg, W. H., *Appl. Surface Sci.* **1**, 25 (1977).

18. Kanski, J., and Rhodin, T. N., *Surface Sci.* **65**, 63 (1977).

19. Campbell, C. T., and White, J. M., *Appl. Surface Sci.* **1**, 347 (1978).

20. Hagen, D. I., Nieuwenhuys, B. E., Rovicka, G., and Somorjai, G. A., *Surface Sci.* **57**, 632 (1976).